ELSEVIER

Journal of Alloys and Compounds 330–332 (2002) 169–174

Journal of ALLOYS AND COMPOUNDS

www.elsevier.com/locate/jallcom

Structure and magnetic properties of TbNiAl-based deuterides

H.W. Brinks[a], V.A. Yartys[a,*], B.C. Hauback[a], H. Fjellvåg[b]

[a]*Institute for Energy Technology, P.O. Box 40, N-2007 Kjeller, Norway*

[b]*Department of Chemistry, University of Oslo, P.O. Box 1033 Blindern, N-0315 Oslo, Norway*

Abstract

This work concerns the study of the crystal and magnetic structure of $TbNiAlD_x$ compounds (x=0.54, 1.23 and 1.33) by neutron diffraction. $TbNiAlD_{0.54}$ is isostructural with TbNiAl. It undergoes two magnetic transitions at T_1=16 K and T_N=36 K, with magnetic structure similar to that of TbNiAl below T_1=23 and T_N=45 K. $TbNiAlD_{1.23}$ is in crystallography and magnetism comparable to $TbNiAlD_{1.1}$. When the Tb_2NiAl positions are occupied, an orthorhombic distortion is induced. This completely changes the magnetic ordering and could be explained by the easy magnetisation directions being perpendicular to the shortest Tb–Tb distances.

Keywords: Magnetic structure; Terbium nickel aluminium deuteride; Crystal structure; Metal hydride; Neutron diffraction

1. Introduction

On hydrogenation of intermetallic compounds, the crystal structure is typically principally retained for the metal sublattice, even though the unit-cell volume may increase by some 10–25%. In some systems several phases are observed, distinguished by symmetry changes due to distortions or changes in filling interstices. Introduction of hydrogen into intermetallic compounds perturbs the crystal structure of the metal sublattice, and the hydrogen atoms are normally considered to donate electrons to the electronic band structure. This influences the electronic and magnetic properties. Often a weakening of the magnetic ordering takes place, e.g. for RNiAl (R=rare earth) [1].

RNiAl for most R takes the ZrNiAl-type structure [2]. Several of these form hydrides with 1.2–1.6 hydrogen per formula unit at ambient temperature and pressure [3]. $TbNiAlD_x$ is saturated at x=1.4, but intermediate phases with x=1.1 and x=0.3 have been synthesised [3]. At low deuterium content the symmetry is hexagonal like TbNiAl, but higher deuteration gives an orthorhombic distortion (*Amm*2): $\mathbf{a}_o=\mathbf{c}_h$, $\mathbf{b}_o=2\mathbf{a}_h+\mathbf{b}_h$, $\mathbf{c}_o=\mathbf{b}_h$ (unit-cell dimensions: $\sim c_h$, $\sqrt{3}a_h$, a_h).

The antiferromagnetic ordering of Tb in TbNiAl is determined below the Néel temperature T_N=45 K as well as below the magnetic order–order transition at T_1=23 K. At 5 K, neutron diffraction experiments prove that 2/3 of the Tb atoms are ordered with propagation vector $\mathbf{k}=(\frac{1}{2},0,\frac{1}{2})$ and 1/3 with propagation vector $\mathbf{k}'=(\frac{1}{2},\frac{1}{2},0)$ or $\mathbf{k}''=(-\frac{1}{2},\frac{1}{2},\frac{1}{2})$, with equally large moments (~7.9 μ_B) along $\mathbf{c}_{hex}$ [4]. Above 10 K, the moments of the latter sublattice decrease quickly (relative to the former) and are ~1 μ_B in size above T_1 [5]. Between T_1 and T_N both orbits have propagation vector **k** with moments along **c** [4].

The magnetic ordering temperature tends to decrease with increasing deuteration (TbNiAl, 45 K; $TbNiAlD_{0.3}$, 42 K; $TbNiAlD_{1.10}$, 11 K; $TbNiAlD_{1.40}$, 14.5 K) [1,4,6,7]. Powder neutron diffraction (PND) studies at 7 and 28 K have shown that $TbNiAlD_{0.3}$ takes the high-temperature magnetic structure of TbNiAl [6]. In $TbNiAlD_{0.8}$, studied as a two-phase mixture, reflections of magnetic origin are observed in the PND pattern below 20 K, and they can partially be indexed on a unit cell with doubling of the orthorhombic **a** and **b** axes [8]. For $TbNiAlD_{1.1}$, the complete magnetic structure is determined: $\mathbf{k}=(0,\frac{1}{2},\frac{1}{2})$ with the magnetic moments in the **bc** plane; i.e. perpendicular to that of the hexagonal structures [7]. For $TbNiAlD_{1.28}$, magnetic reflections, which are in correspondance with the magnetic structure of $TbNiAlD_{1.10}$, are present in the PND pattern below 16 K [8].

The present study describes the crystal structure and magnetism of $TbNiAlD_{0.54}$, $TbNiAlD_{1.23}$ and $TbNiAlD_{1.33}$, and the extended knowledge is summarised in an overall presentation for the $TbNiAlD_x$ system.

*Corresponding author. Tel.: +47-63-806-453; fax: +47-63-812-905.
E-mail address: Volodymyr.Yartys@ife.no (V.A. Yartys).

0925-8388/02/$ – see front matter
PII: S0925-8388(01)01644-9

2. Experimental

TbNiAl was prepared from Tb (purity 99.8%), Ni (99.9%) and Al (99.9%) by arc melting in an argon atmosphere. The ingots were remelted several times to increase their homogeneity, with subsequent annealing for 2 weeks at 600°C. X-ray powder diffraction (Siemens D5000, Cu $K\alpha_1$ radiation, Bragg–Brentano geometry, primary monochromator, position sensitive detector, Si internal standard) confirmed formation of single-phased TbNiAl with ZrNiAl-type structure [$a=6.9992(6)$ and $c=3.8801(7)$ Å]. After activation in vacuum at 300°C, the sample was deuterated at room temperature and $p_{D_2}=4$ bar. This saturated sample contained (after replacing the D_2 atmosphere with Ar) 1.23 D per formula unit. Vacuum desorption at 120°C gives $TbNiAlD_{0.54}$. $TbNiAlD_{1.33}$ was synthesized in-situ at the neutron diffraction beam line at $p_{D_2}=4$ bar. D contents refer to results derived by Rietveld refinements.

PND data were collected with the PUS instrument at the JEEP II reactor, Kjeller, Norway. The experimental setup consisted of a focusing Ge(511) monochromator, a 5-mm cylindrical sample holder, a Displex cooling system controlled by an Oxford controller and two banks of seven position-sensitive ^{3}He detectors, each covering 20° in 2θ ($\Delta 2\theta=0.05°$). PND data from 10 to 130° were collected at 293 K and from 4 to 130° at lower temperature. Fullprof [9] was used for Rietveld refinements with Pseudo–Voigt profiles, manually set background points and scattering lengths taken from the library of the program.

Magnetic susceptibility was measured by a SQUID device (Magnetic Property Measurement System, Quantum Design) on free powder in a gelatin capsule. Calibration was carried out by means of a Pd standard (from NIST).

3. Results

3.1. Structure and magnetism of $TbNiAlD_{0.54}$

PND data of $TbNiAlD_{0.54}$ revealed a hexagonal structure isostructural with the alloy. Deuterium occupy 80% of the bipyramidal site which is surrounded by Tb_3Ni_2, and there are no signs of any ordered filling of D, contrary to $TbNiAlD_{0.32}$ [6]. The refined structural parameters and reliability factor for the data at $T\leq 293$ K are given in Table 1. The thermal expansion is very anisotropic (a: +1.0%, c: −1.3% from 7 to 293 K), whereas the volume-expansion coefficient is normal, $\alpha_V=2.2\cdot 10^{-5}$ (V increase: +0.63%). PND experiments at intermediate temperatures reveal a gradual increase of c upon cooling, which exclude the interlayer contraction to be explained by magnetostriction below the Néel temperature.

The magnetic susceptibility versus temperature curve shows two maxima (Fig. 1) at 16 and 36 K. Above 80 K, Curie–Weiss behaviour is observed. PND at 22 and 7 K reveal magnetic ordering, with slightly different ordering schemes, cf. Fig. 1. The effect at 36 K probably corresponds to T_N, whereas $T_1=16$ K (vide supra). The magnetic moments of Tb at 7 K are 8.1 and 7.3 μ_B on the two sites, somewhat below the theoretical value 9 μ_B for Tb^{3+}. At 22 K, the corresponding ordered magnetic moments are 7.7 and 1.20 μ_B, revealing a frustration of μ_{Tb2} at elevated temperatures, similar to that observed for the intermetallic compound.

Table 1
Crystallographic[a] and magnetic data for $TbNiAlD_{0.54}$ derived from Rietveld analysis of PND data, calculated standard deviations in parentheses; the magnetic arrangement at 7 and 22 K was based on low and high temperature model of TbNiAl, respectively

	7 K	22 K	293 K
a	7.0270(2)	7.0257(2)	7.0931(5)
c	3.9685(3)	3.9615(3)	3.9174(2)
x_{Tb}	0.5862(7)	0.5866(6)	0.5878(4)
x_{Al}	0.2331(14)	0.2334(13)	0.2372(7)
B_{Tb}	0.48(4)	0.38(5)	0.47(4)
B_{Ni1}	1.20(8)	1.04(7)	1.29(5)
B_{Ni2}	0.59(14)	0.64(9)	0.75(5)
B_{Al}	1.04(17)	0.76(14)	0.49(8)
B_D	3.4(2)	3.6(2)	2.7(1)
$\mu_{z,Tb1}$	8.1(7)	7.7(7)	–
$\mu_{z,Tb1}$	7.3(7)	1.20(13)	–
R_M	9.0	11.6	–
R_p	6.9	6.7	4.0
χ^2	7.9	8.2	2.6

[a] Space group $P\bar{6}2m$ (≠189). Tb in 3*g*, Ni1 in 2*c*, Ni2 in 1*b*, Al in 3*f* and D in 2*d*. $n_D=0.815(12)$.

3.2. Structure and magnetism of $TbNiAlD_{1.23}$ and $TbNiAlD_{1.33}$

$TbNiAlD_{1.23}$ and $TbNiAlD_{1.33}$ are isostructural with the orthorhombically distorted $TbNiAlD_{1.1}$. The refinements show that one Tb_3Ni_2 (denoted D1) and two Tb_2NiAl (D2 and D3) sites are occupied by deuterium. The results of the refinements are shown in Table 2.

From susceptibility data, $T_N=14$ K was established. PND measurements at 7 K, show that the magnetic moments are ordered in the orthorhombic **bc** plane (perpendicular to $\mathbf{c}_{hex}$). The ordering (cf. Fig. 2) is closely related to that described for $TbNiAlD_{1.10}$ with Tb1 ordered (9.2 μ_B) along Tb-chains in the **b** direction, and Tb2 ordered (5.4 μ_B) pointing along **c**.

3.3. Nuclear structure of $TbNiAlD_x$

At low deuterium content, D occupies Tb_3Ni_2 positions. This leads to an expansion of all hexagonal unit-cell dimensions. For $TbNiAlD_{0.32}$, which is stable to relatively high temperature, there is an ordering of half-filled D on the Tb_3Ni_2 site. This gives a superstructure with doubled c axis [6].

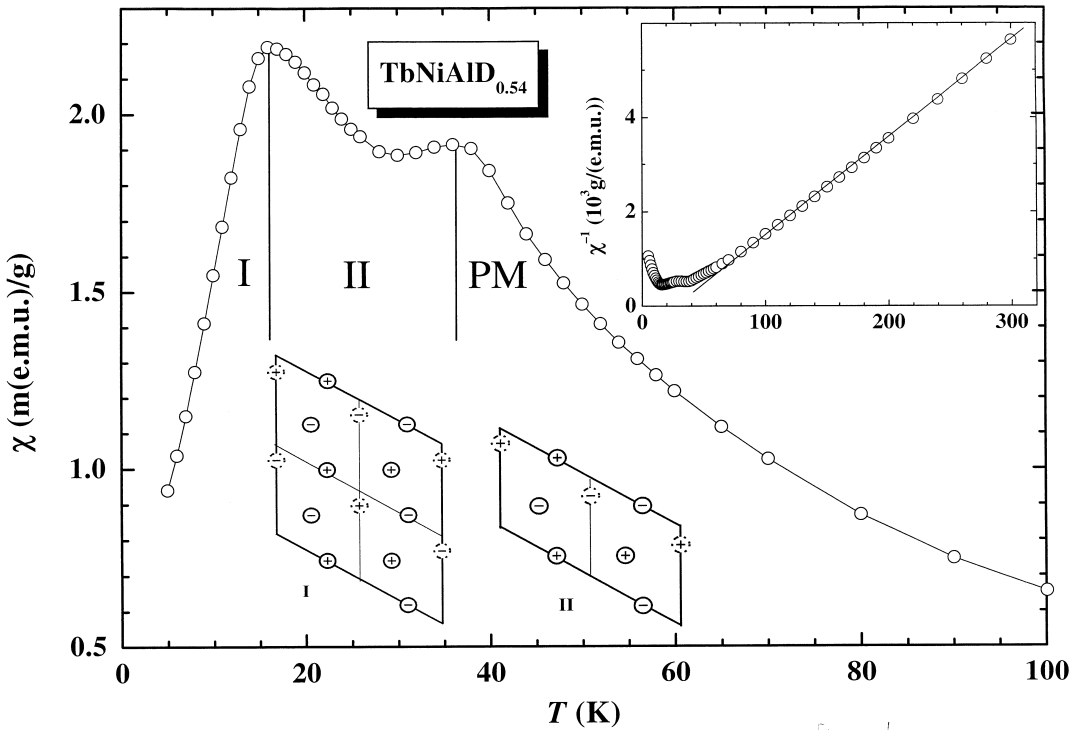

Fig. 1. Magnetic susceptibility of $TbNiAlD_{0.54}$. Temperature regions of the two different ordered magnetic arrangements and paramagnetism (PM) are marked. Inset shows inverse magnetic susceptibility for $T \leq 300$ K.

Table 2
Crystallographic[a] and magnetic data for $TbNiAlD_{1.23}$ derived from Rietveld analysis of PND data, calculated standard deviations in parentheses, unit-cell dimensions of $TbNiAlD_{1.33}$ at 293 K are $a = 3.7428(6)$, $b = 12.3607(15)$, $c = 7.6210(15)$ Å

	7 K	293 K
a	3.6689(2)	3.7094(2)
b	12.3714(4)	12.3784(5)
c	7.6583(4)	7.6379(4)
y_{Tb1}	0.2134(4)	0.2105(3)
z_{Tb1}	0.0525(14)	0.0454(11)
z_{Tb2}	0.661(2)	0.6524(13)
y_{Ni1}	0.3297(4)	0.3307(3)
z_{Ni1}	0.2835(15)	0.2777(12)
z_{Ni2}	0.2532(15)	0.2479(12)
y_{Al1}	0.1198(12)	0.1196(9)
z_{Al1}	0.340(2)	0.3345(15)
z_{Al2}	0.0000(–)	0.0000(–)
y_{D1}	0.3313(6)	0.3321(4)
z_{D1}	0.280(2)	0.2672(15)
y_{D2}	0.3797(6)	0.3819(5)
z_{D2}	0.084(2)	0.0769(13)
y_{D3}	0.2410(–)	0.2410(–)
z_{D3}	0.4020(–)	0.4020(–)
$\mu_{y,Tb1}$	3.2(3)	–
$\mu_{z,Tb1}$	8.6(9)	–
$\mu_{z,Tb2}$	5.4(6)	–
R_M	9.4	–
R_p	5.5	3.5
χ^2	4.8	3.4

[a] Space group *Amm*2 (#38). Tb1 in 4*e*, Tb2 in 2*b*, Ni1 in 4*d*, Ni2 in 2*b*, Al1 in 4*d*, Al2 in 2*a*, D1 in 4*e*, D2 and D3 in 4*d*. $n_{D1} = 0.946(12)$, $n_{D2} = 0.864(13)$, $n_{D3} = 0.033(11)$.

When the D content exceeds the amount of available Tb_3Ni_2 positions, D also occupies two different Tb_2NiAl sites, D2 and to a small extent D3. The geometry around the D2 site is changed considerably upon filling with D, which gives considerable shortening of the Tb–Tb distances ($\|\mathbf{c}_h$ or $\|\mathbf{a}_o$) and elongation of Ni–Al distances ($\|\mathbf{b}_h$ or $\|\mathbf{c}_o$). This size mismatch of the D2 site induces a distortion of the lattice, lowering the symmetry to orthorhombic. In terms of the orthorhombic superstructure, the variation of the unit-cell dimensions could be followed for the whole $TbNiAlD_x$ system, see Fig. 3. Whereas insertion of the first 0.54 D per formula unit gives an increase in each unit-cell parameter by approximately 1%, the next insertion of additional 0.56 D results in -6% for a_o, $+7\%$ for c_o and $+1\%$ for b_o. Notably, the unit-cell volume remain roughly unchanged during the distortion, inset to Fig. 3.

3.4. Magnetism of $TbNiAlD_x$

The magnetic susceptibility as well as magnetic ordering by PND have been studied for $TbNiAlD_x$, $x \leq 1.23$. The magnetic ordering is antiferromagnetic in low magnetic fields. At higher fields TbNiAl also undergoes a metamagnetic transition at 0.4 T. T_N tends to decrease upon deuteration. Three different antiferromagnetic regimes exist, two of the orderings are associated with the hexagonal crystal symmetry and the third with the orthorhombic

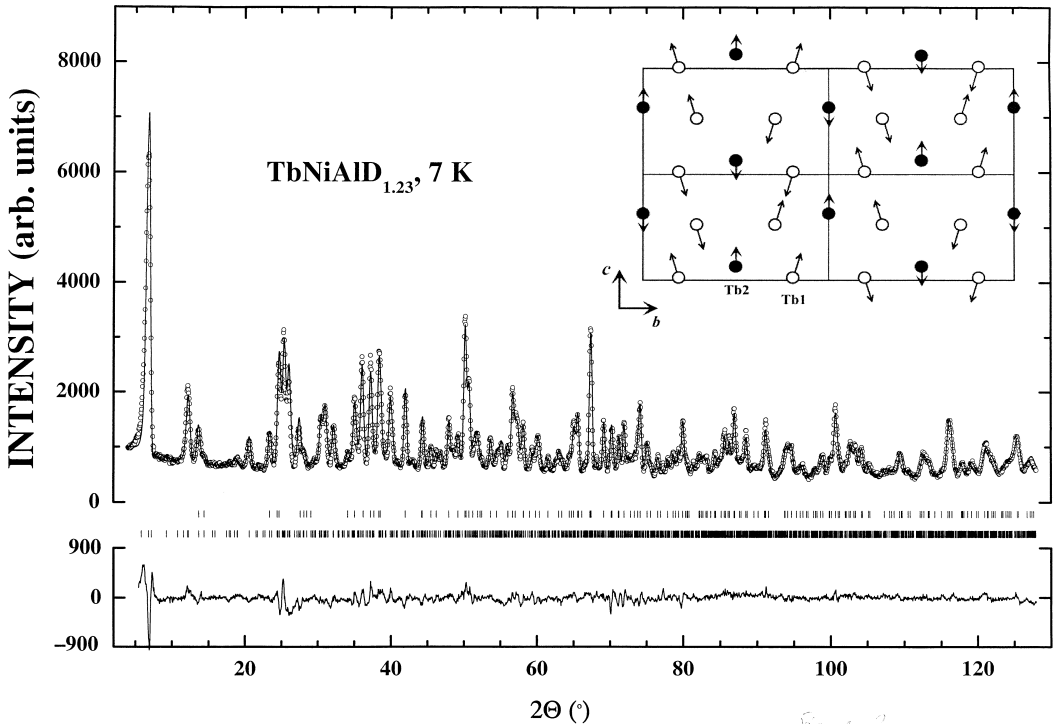

Fig. 2. Rietveld refinements (upper line) of PND data (circles) for $TbNiAlD_{1.23}$ at 7 K. Positions of Bragg reflections are shown with bars for the nuclear (upper) and magnetic (lower) contribution. The difference between observed and calculated intensity is shown with the bottom line. The refined magnetic arrangement is shown in the inset.

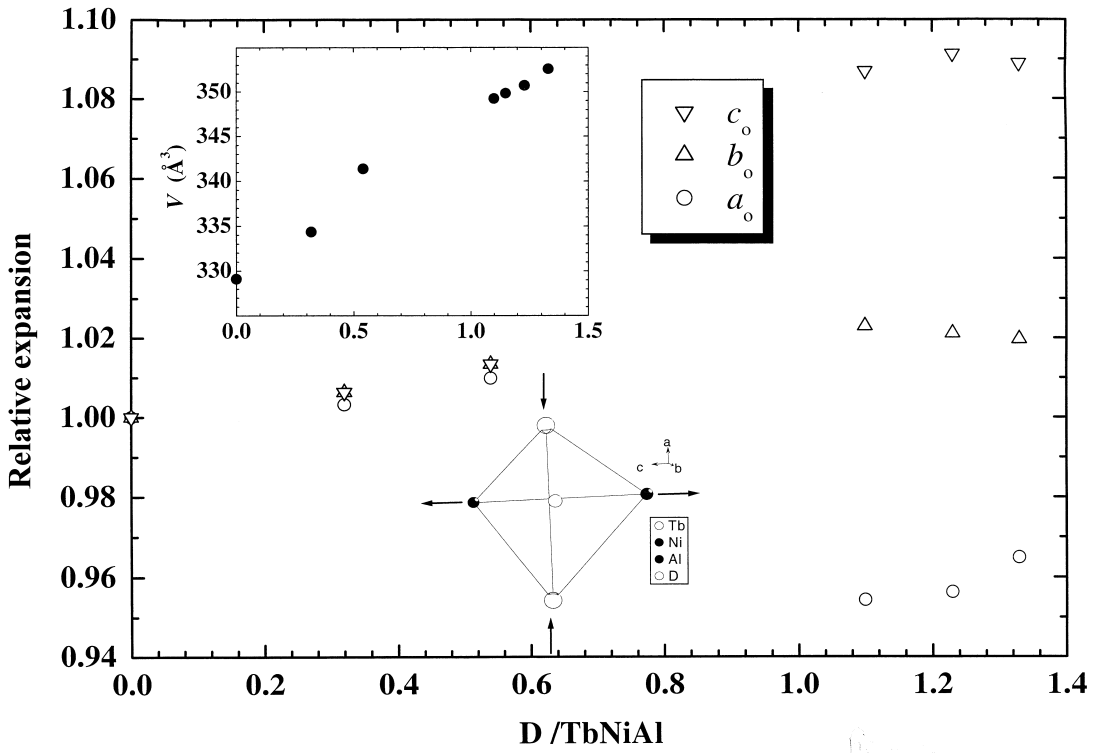

Fig. 3. Relative expansion of the unit-cell dimensions of $TbNiAlD_x$, according to the superstructure model. Variation of the unit-cell volume shown in inset. The distortion of the Tb_2NiAl tetrahedra leading to the orthorhombic distortion is illustrated.

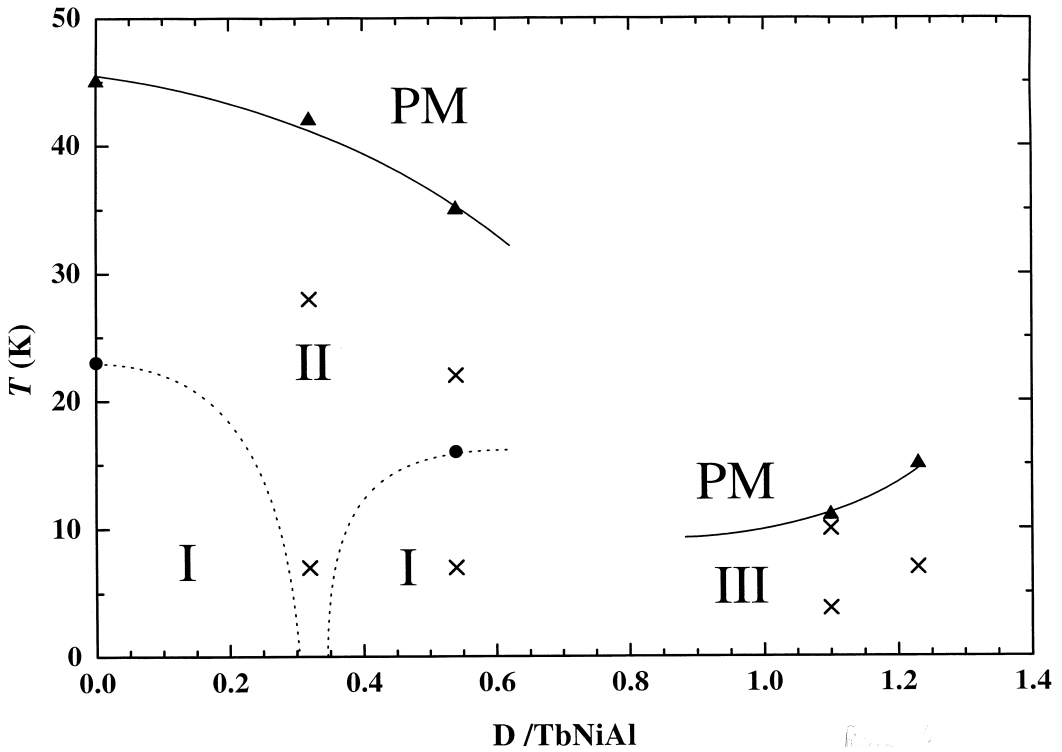

Fig. 4. Magnetic phase diagram (temperature versus composition) of $TbNiAlD_x$ determined from magnetic susceptibility and PND. Experimental PND experiments are shown by crosses.

symmetry. The magnetic phase diagram is schematically drawn in Fig. 4.

The distortion resulting in the structural transition to the orthorhombic symmetry also modifies the magnetic structure. In the hexagonal structure of $TbNiAlD_x$, the magnetic moments are ordered along $\mathbf{c}_h$, whereas the magnetic moments in the orthorhombic structure are ordered perpendicular to $\mathbf{c}_h$. This is in line with the findings of Nakotte [10], who states that in U*TX* compounds (*T* = Transition metal, *X* = P-block element) of several structure types (ZrNiAl, TiNiSi and LiGaGe), the easy magnetic directions or planes are perpendicular to the nearest inter-uranium distance. As shown in Table 3, the shortest Tb–Tb distance change from being within $\mathbf{a}_h\mathbf{b}_h$ plane in the hexagonal symmetry to be perpendicular to such planes in the orthorhombic symmetry.

Table 3
Selected interatomic distances in Å for $TbNiAlD_x$, $x = 0$ (atomic coordinates from Ref. [5] and unit-cell dimensions from Ref. [7]), 0.32 (Ref. [6]), 0.54 (present), 1.1 (Ref. [7]) and 1.23 (present)[a]

		TbNiAl	$TbNiAlD_{0.32}$	$TbNiAlD_{0.54}$	$TbNiAlD_{1.1}$	$TbNiAlD_{1.23}$
D1	Tb–Tb	3.645	3.826	3.707	3.699; 3.936; 3.953	3.676; 3.942; 3.975
	Tb–Ni	2.862	2.880	2.902	2.812; 2.938; 2.967	2.807; 2.958; 2.967
	D–Tb	–	2.209	2.140	2.197; 2.225; 2.282	2.189; 2.256; 2.266
	D–Ni	–	1.848	1.959	1.853	1.857
D2	Tb–Tb	3.879	3.895	3.917	3.702	3.709
	Tb–Ni	2.862	2.880; 2.888	2.901	2.938	2.958
	Tb–Al	3.185	3.149; 3.228	3.209	3.369	3.395
	Ni–Al	2.757	2.760	2.769	3.389	3.441
	D–Tb	–	–	–	2.422	2.431
	D–Ni	–	–	–	1.602	1.659
	D–Al	–	–	–	1.856	1.852
$D–D_{min}$		–	5.628	3.917	2.395	2.400
Tb–Tb intra-plane		3.645	3.535; 3.826	3.707	3.699; 3.936; 3.953	3.676; 3.942; 3.975
Tb–Tb inter-plane		3.879	3.895	3.917	3.702	3.709

[a] For comparison, shortest Al–D distance is 1.86 Å in AlD_3 [11], shortest Ni–D distance is 1.71 in $NiD_{0.73}$ at 80 K [12] shortest Tb–D distances are 2.24 and 2.28 Å in $TbD_{2.23}$ at 70 K [13].

The idea that short distances lead to perpendicularly ordered magnetic moments works well in predicting whether the magnetic moments are ordered parallel or perpendicular to the $\mathbf{a}_h\mathbf{b}_h$ planes. To a certain degree this coupling could also explain the magnetic ordering in larger detail. In $TbNiAlD_{1.1}$, the magnetic moment of Tb1 is nearly perpendicular to the nearest Tb (Tb2 at 3.699 Å) and parallel to Tb1 at larger distance (3.936 Å). Similar arguments appear to prevail for Tb2. Furthermore, for $TbNiAlD_{0.32}$, there is a corner-sharing network of Tb triangles with alternating short-edged and long-edged triangles. With an antiferromagnetic coupling at short distances, such a geometry necessarily leads to frustration. This is indeed observed, with $\mu_{Tb1} = 8.0$ and $\mu_{Tb2} = 1.3\ \mu_B$ [6].

4. Concluding remarks

The system $TbNiAlD_x$ undergoes two structural changes that strongly influence the magnetic properties. There is an ordering of D at 50% occupation of the Tb_3Ni_2 site, which gives different (filled or empty) Tb_3Ni_2 polyhedra and altered magnetic ordering.

When the Tb_3Ni_2 site is fully occupied, geometrically less suited Tb_2NiAl sites become occupied. This results in a considerable distortion of the structure away from the hexagonal symmetry of TbNiAl to orthorhombic symmetry. The magnetic ordering at low temperature is accordingly completely different.

The orthorhombic distortion take place for all $RNiAlD_x$ (R = Sm, Gd, Y, Tb, Dy, Ho, Er) at high deuteration level, but not for $LuNiAlD_{1.00}$ [14,15]. For Y and Er the distortion starts at a deuteration level above 0.67. Unfortunately, there are no structural data available for those compounds, and it is hence not possible to compare the distortion around the D2 site on increasing deuterium content.

A summary of the crystal structure and magnetic orderings of $TbNiAlD_x$ is given in Fig. 5.

References

[1] A.V. Kolomiets, L. Havela, V.A. Yartys, A.V. Andreev, J. Alloys Comp. 253 (1997) 343.
[2] E.I. Hladyshevskiy, O.I. Bodak, Crystal Chemistry of Intermetallic Compounds of Rare Earth Metals, Vyszcza Shkola, Lviv, 1982.
[3] V.A. Yartys, F. Gingl, K. Yvon, L.G. Akselrud, A.V. Kolomietz, L. Havela, T. Vogt, I.R. Harris, B.C. Hauback, J. Alloys Comp. 279 (1998) L4.
[4] P. Javorsky, P. Burlet, V. Sechovsky, A.V. Andreev, J. Brown, P. Svoboda, J. Magn. Magn. Mater. 166 (1997) 133.
[5] G. Ehlers, H. Maletta, Z. Phys. B 99 (1996) 145.
[6] B.C. Hauback, H. Fjellvåg, L. Pålhaugen, V.A. Yartys, K. Yvon, J. Alloys Comp. 295 (1999) 178.
[7] H.W. Brinks, V.A. Yartys, B.C. Hauback, H. Fjellvåg, K. Yvon, F. Gingl, T. Vogt, J. Alloys Comp. 311 (2000) 114.
[8] H.N. Bordallo, H. Nakotte, J. Eckert, A.V. Kolomiets, L. Havela, A.V. Andreev, H. Drulis, W. Iwasieczko, J. Appl. Phys. 83 (1998) 6986.
[9] J. Rodríguez-Carvajal, FULLPROF version 0.2, LLB, Saclay, 1998.
[10] H. Nakotte, Thesis, Magnetism in Cerium and Uranium Intermetallics, Freie Universiteit, Amsterdam, 1994.
[11] J.W. Turley, H.W. Rinn, Inorg. Chem. 8 (1969) 17.
[12] V.P. Zhebelev, V.A. Somenkov, E.G. Ponyatovskii, S.S. Shil'shtein, I.T. Belash, Neorg. Mat. 14 (1978) 1620.
[13] Q. Huang, T.J. Udovic, J.J. Rush, J. Schefer, I.S. Anderson, J. Alloys Comp. 231 (1995) 95.
[14] A.V. Kolomiets, L. Havela, V. Sechovsky, A.V. Andreev, V.A. Yartys, I.R. Harris, Int. J. Hydrogen Energy 24 (1999) 119.
[15] V.A. Yartys, Unpublished results.

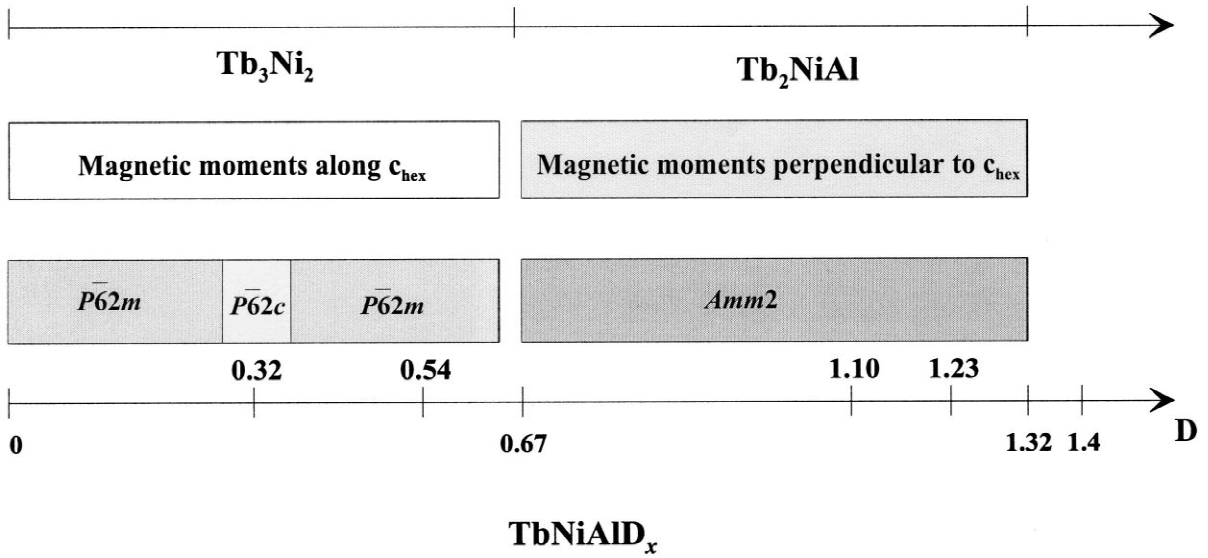

Fig. 5. Occupied deuterium sites, symmetry and magnetism of $TbNiAlD_x$.